Supplemental Figures and Legends

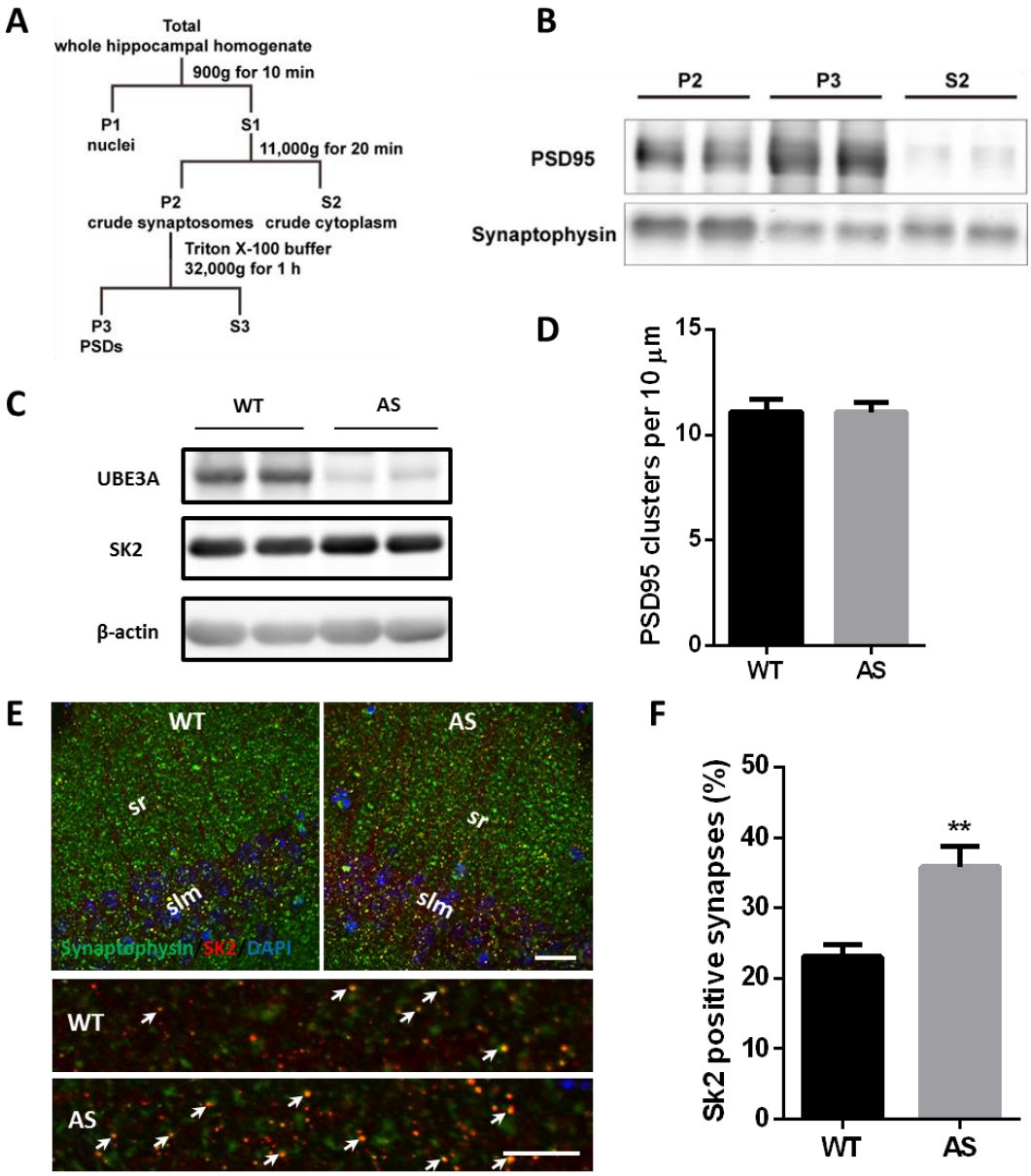

Figure S1. Characterization of SK2 expression in hippocampus of AS and WT mice, Related to Figure 1

(**A**) Schematic of hippocampal tissue fractionation by differential centrifugation.

(**B**) Characterization of different fractions: Equal amounts of protein from P2, P3 and S2 fractions were probed for the synaptic vesicle marker synaptophysin, and the postsynaptic density marker PSD95.

(**C**) Levels of UBE3A and SK2 in whole hippocampal homogenates from WT or AS mice. β-actin was used as loading control.

(**D**) Quantitative data of the number of PSD95-immunoreactive puncta in hippocampal CA1 region of WT and AS mice. Unpaired two-tail t-test, $p > 0.05$, N = 18-24 regions of interest from at least 9 slices from at least 3 mice per group.

(**E**) Upper panel: Representative images of stratum radiatum (sr) in hippocampal CA1 region of WT and AS mice stained with anti-SK2 (red) and anti-synaptophysin (green) antibodies. slm, stratum lacunosum moleculare. Scale bar = 20 μm. Lower panel: High magnification images of SK2- and synaptophysin-immunopositive puncta (arrows) along apical dendrites of hippocampal pyramidal neurons. Scale bar = 10 μm.

(**F**) Quantitative analysis of the percent of SK2- and synaptophysin-dually labeled puncta, normalized to the total number of synaptophysin-labeled puncta. Images similar to those shown in (E) were taken blindly with a 100x objective from 20 sections per mouse and a total of 3 mice. Puncta in an area of 500 μm^2 were quantified using ImageJ and shown are means ± S.E.M. ** $p < 0.01$; unpaired two-tail t-test.

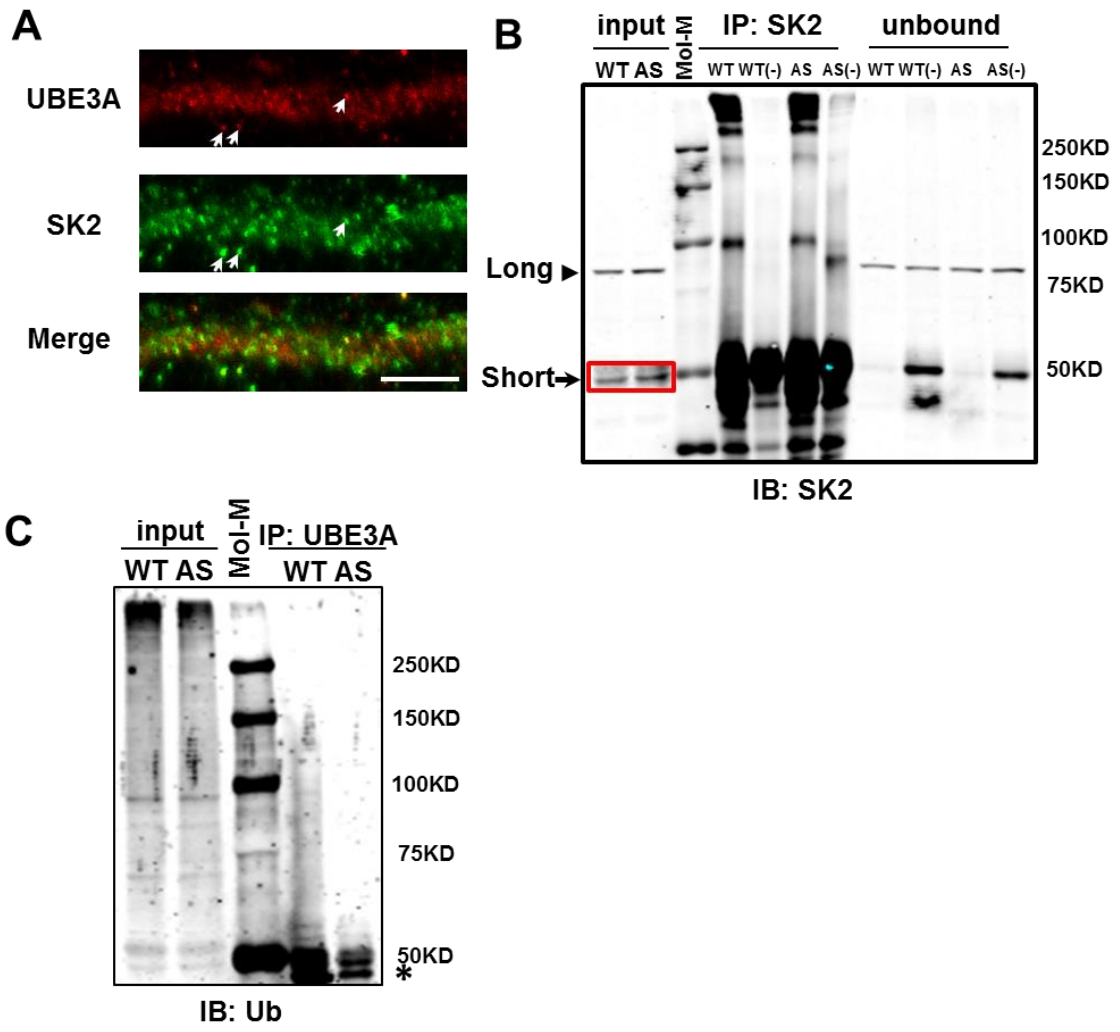

Figure S2. Interaction between UBE3A and SK2, Related to Figure 2

(**A**) Partial co-localization of UBE3A and SK2 in dendritic spines of a DIV15 neuron cultured from a WT mouse (arrows indicate clear co-localized expression). Scale bar= 5 μm.

(**B**) Immunoprecipitation of hippocampal crude synaptosome fractions from either WT or AS mice with an anti-SK2 antibody (Santa Cruz) and probed with another anti-SK2 antibody (Aviva). Arrow indicates the short isoform (red box, with enhanced exposure), while arrowhead indicates the long isoform of SK2. Note the presence of high molecular weight bands in the SK2 antibody-pull down fractions, but very little in control IgG (-) fractions. The short isoforms of SK2 overlap with the heavy chain IgG, because antibodies used for

both IP and IB are rabbit IgG. There is no commercially available antibody from a different animal species. However, the lack of short form SK2 band in the “unbound” fractions indicates the specific pull-down of this isoform by the antibody. Mol-M, molecular weight marker.

(**C**) Immunoprecipitation of hippocampal membrane fractions from either WT or AS mice with an anti-UBE3A antibody and probed with anti-ubiquitin antibodies. *, heavy chain IgG.

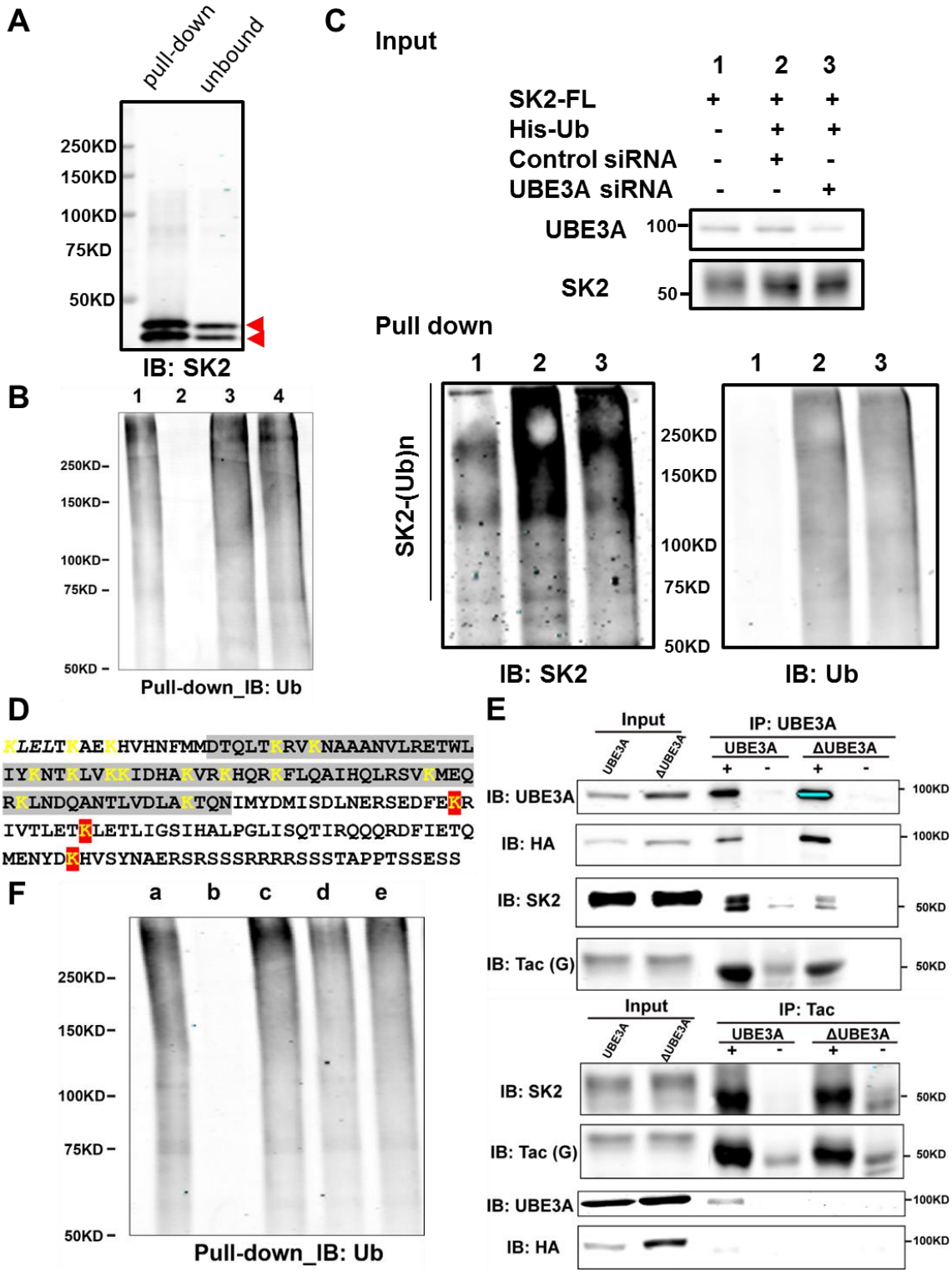

Figure S3. ***In vitro*** **ubiquitination assay and His-ubiquitin pull down analyses of SK2 ubiquitination, Related to Figure 3**

(**A**) GST-SK2 C-terminal (SK2-C) fusion proteins were expressed in *E. coli*, extracted and then purified using a Pierce Glutathione Agarose product. Pull-down fractions and unbound fractions were analyzed by Western blotting using SK2 antibody. Original bands of SK2-C are indicated by arrowheads.

(**B**) His-ubiquitin pull down assay performed following UBE3A siRNA treatment. Levels of ubiquitin were determined by Western blot analysis. (1) only His-ubiquitin, (2) only Tac-SK2, (3) His-Ub and Tac-SK2 plus control siRNA, (4) His-Ub and Tac-SK2 plus UBE3A siRNA. This image is paired with Figure 3B.

(**C**) His-ubiquitin pull down assay performed using full-length SK2 (SK2-FL). Upon purification, levels of ubiquitinated SK2-FL protein (lower left panel) and ubiquitin (lower right panel) were determined by Western blot analysis. Upper panel, input of UBE3A and SK2.

(**D**) Candidate UBE3A ubiquitination sites (red) within SK2 C-terminus. Calmodulin-binding domain (CaMBD), highlighted in grey.

(**E**) Interaction between SK2 and UBE3A. Upper panel: Cell lysates were immunoprecipitated with an anti-UBE3A antibody or control IgG and probed with the indicated antibodies. Anti-HA antibody was used to confirm the presence of the gene products (HA-UBE3A or HA-ΔUBE3A). The presence of Tac-SK2 in precipitates was confirmed with anti-SK2 and anti-Tac antibodies. Lower panel: Cell lysates were immunoprecipitated with anti-Tac antibody (mouse) or control mouse IgG and probed with the indicated antibodies. These results indicate that SK2 co-immunoprecipitates with UBE3A and UBE3A is also co-precipitated with SK2.

(**F**) His-ubiquitin pull down assay performed in cells co-transfected with (a) only His-ubiquitin, (b) only Tac-SK2, (c) His-Ub and Tac-SK2 plus UBE3A, (d) His-Ub and Tac-SK2

plus ΔUBE3A, (e) His-Ub and ΔK plus UBE3A. Levels of ubiquitin were determined by Western blot analysis. This image is paired with Figure 3E.

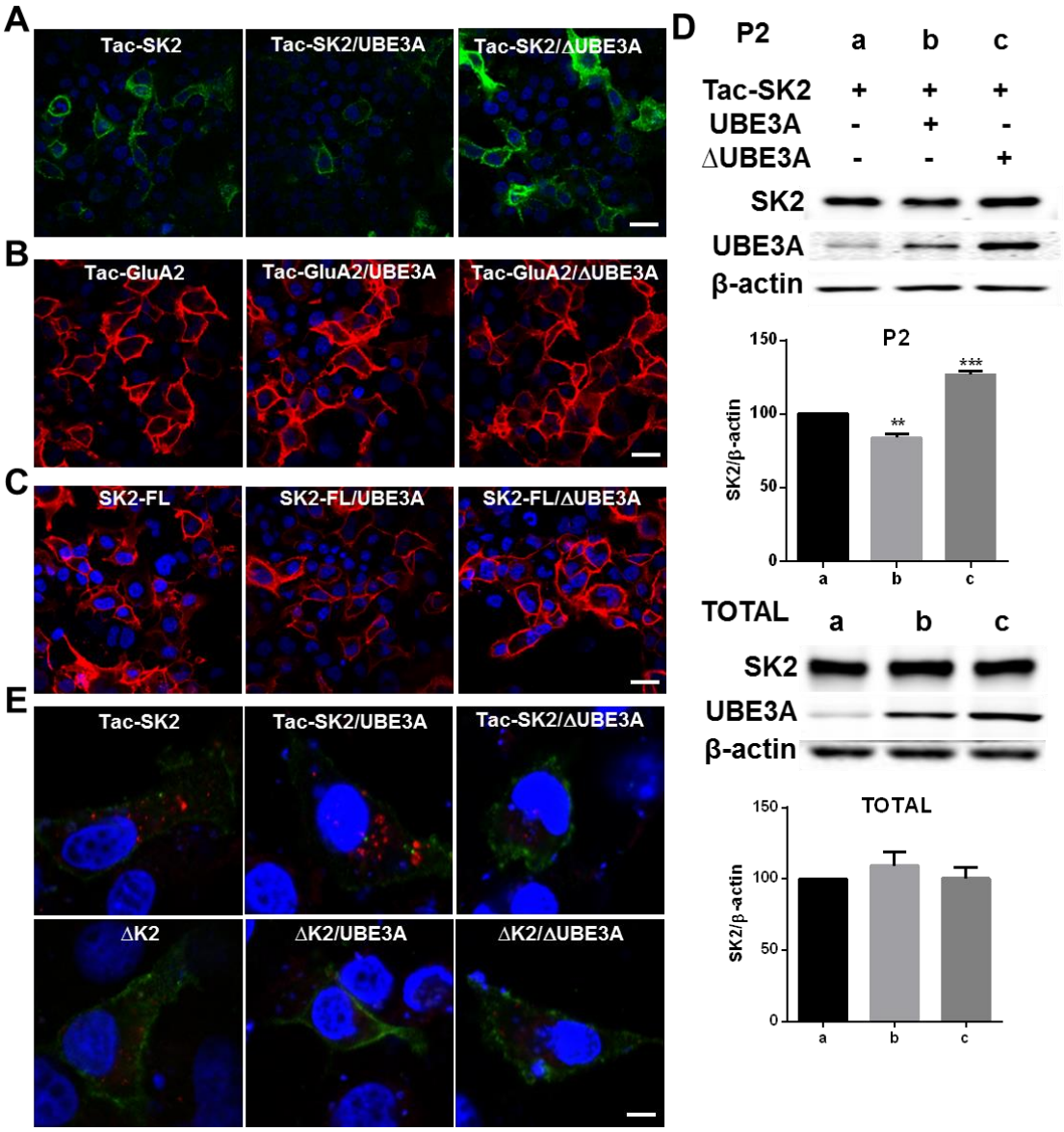

Figure S4. Characterization of Tac-SK2, full-length SK2, Tac-GluA2 surface expression and the effect of K506R/K514R/K550R mutations on SK2 endocytosis, Related to Figure 4

(**A-C**) Low power images of Tac-SK2 (green in **A**), Tac-GluA2 (red in **B**), and SK2-FL (red in **C**) surface expression in COS-1 cells in the presence or absence of UBE3A or ΔUBE3A. Scale bar=30 μm. Blue shows DAPI labeled nuclei.

(**D**) Western blot analysis and quantification of UBE3A and Tac-SK2 expression in crude membrane fraction (P2, upper panel) and whole cell lysates (TOTAL, lower panel) from COS-1 cells; β-actin was used as loading control. Results are means ± S.E.M. $^{**}p < 0.01$, $^{***}p < 0.001$ as compared to Tac-SK2 alone (n=3, one-way ANOVA followed by Newman-Keuls test).

(**E**) Representative images of SK2 endocytosis in cells transfected with either Tac-SK2 (upper panels) or K506R/K514R/K550R (ΔK2) (lower panels), in the presence or absence of either UBE3A or ΔUBE3A. Internalized Tac-SK2/ΔK2 proteins are labeled in red, while surface-expressed are in green. Scale bar=10 μm.

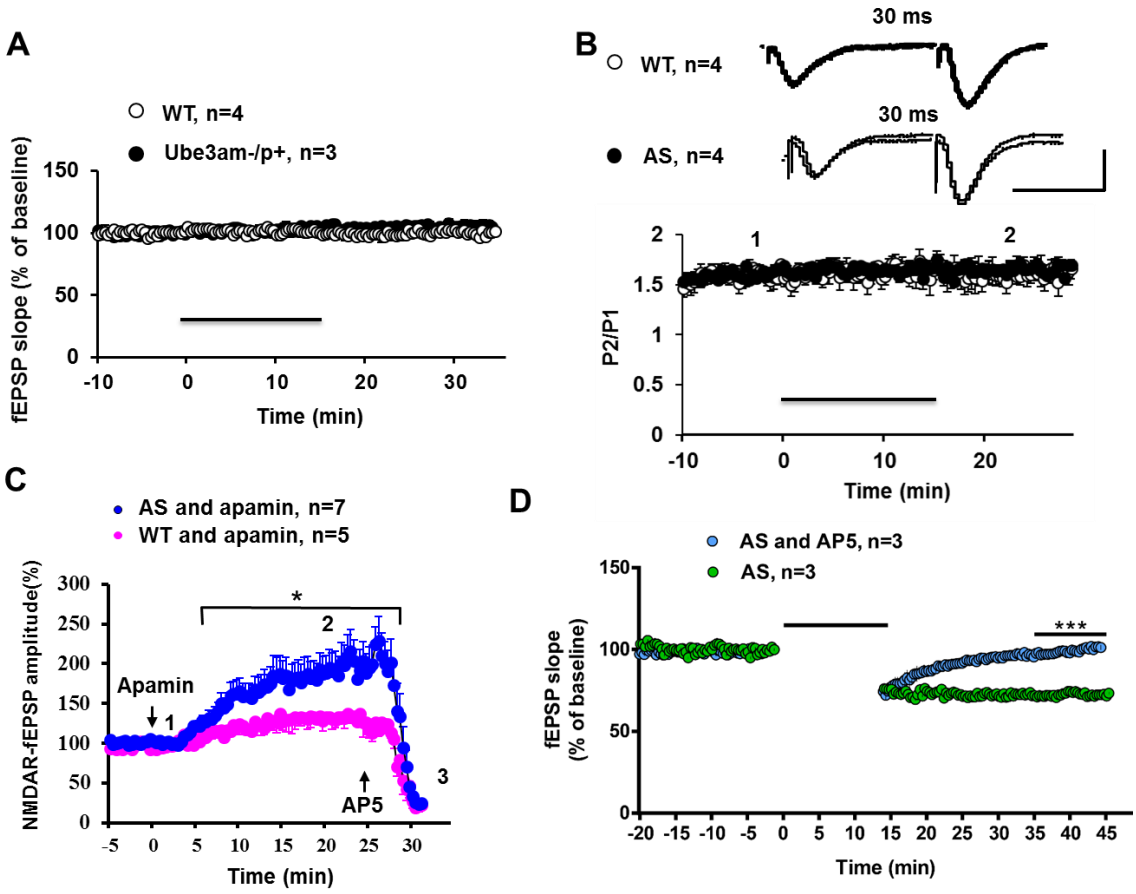

Figure S5. Characterization of the effects of apamin application on basal synaptic transmission and NMDAR-mediated field EPSP, Related to Figure 5

(**A**) Application of 20 nM apamin for 15 min did not affect AMPAR-mediated synaptic transmission.

(**B**) Apamin application did not affect paired-pulse facilitation elicited by 2 stimuli delivered at 30 ms interval. Inserts are representative traces at the time points indicated by 1, 2. The black line indicates apamin application. Scale bar: 0.5 mV/20 ms.

(**C**) Apamin application produced a larger effect on NMDAR-mediated fEPSP in hippocampal slices from AS mice, as compared to WT mice. *$p < 0.05$ (unpaired two-tail t-test). NMDAR-mediated fEPSPs after apamin treatment in AS and WT hippocampal slices are expressed as % of their respective baseline controls (before apamin application).

(**D**) LTD induced by LFS (1 Hz for 15 min) in hippocampal slices from AS mice is blocked by AP5. ***p <0.001 (n=3, one-way ANOVA followed by Bonferroni test).

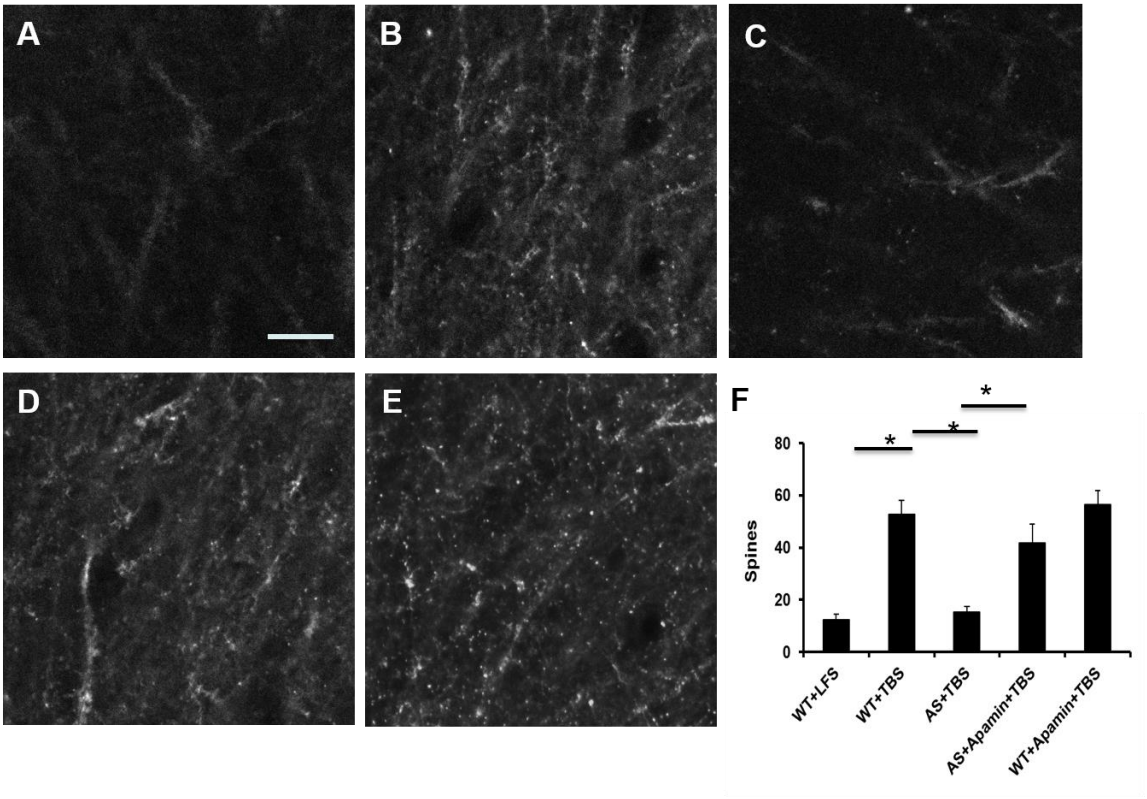

Figure S6. Apamin treatment promotes TBS-induced actin polymerization in hippocampal slices from AS mice, Related to Figure 5

AlexaFluor-tagged phalloidin was topically applied to slices at the conclusion of physiological recording to label filamentous actin (F-actin). Quantification of the number of fluorescent spines was performed with an automated system for a 500 μm^2 sampling zone surrounding the recording electrode.

(**A-E**) Representative images of hippocampal slices from WT mice after LFS (A, WT+LFS), TBS (B, WT+TBS) or TBS with apamin pre-treatment (E, WT + Apamin + TBS) or from AS mice after TBS (C, AS + TBS) or TBS with apamin pre-treatment (D, AS + TBS). Scale bar=10 μm.

(**F**) Quantitative analysis of F-actin staining. Results are means ± S.E.M. *p < 0.05 (n=5 for each experimental groups; two-way ANOVA followed by Bonferroni test).

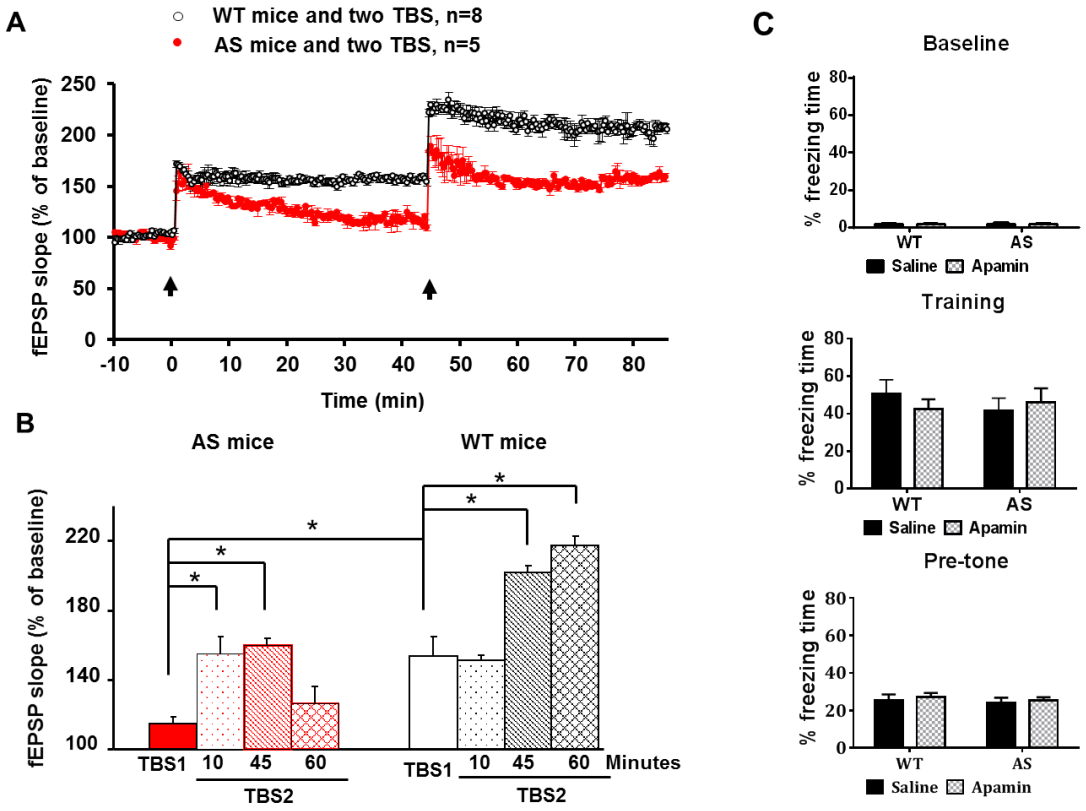

Figure S7. Characterization of LTP properties and basal level freezing in AS and WT mice, Related to Figures 6 and 7

(**A**) Effects of two TBS (arrows) delivered at 45 min interval in hippocampal slices from AS (red) and wild-type (white) mice on LTP.

(**B**) LTP amplitude measured at 40 min post-TBS1 or –TBS2 delivered at different time points after TBS1 in the different groups. Results are means ± S.E.M. * p < 0.05 (n=5-8; two-way ANOVA followed by Bonferroni test).

(**C**) Top panel: Pre-training baseline freezing behavior. Middle panel: Percent freezing of different experimental groups during 30 sec after the 3rd footshock. Bottom panel: Pre-tone testing freezing behavior.

Supplemental Experimental Procedures

Mice

Mice were housed in groups of 2-3 per cage on a 12-h light/dark cycle, with food and water available ad libitum.

DNA Constructs

Expression constructs encoding HA-UBE3A, HA-UBE3A-C833A (catalytically inactive) were obtained from Addgene (Talis et al., 1998). Expression construct encoding Tac-SK2 C-terminus was generated by PCR-based approaches. Constructs with K-A or K-R mutations (ΔK or ΔK2) were generated from Tac-SK2 by site-directed mutagenesis (IDT). Full-length SK2 with triple-myc epitope (SK2-FL) and GST-SK2 carboxyl-terminal (SK2-C) constructs were gifts from Dr. John Adelman (Strassmaier et al., 2005).

Transfection and Antibodies

For transient expression, cells were transfected with the respective constructs by lipofection (Lipofectamine 2000; Invitrogen). Small interfering RNA (siRNA) transfections were also performed with Lipofectamine 2000. Cells were incubated with 10- or 20-nM SMARTpool siRNA against human *UBE3A*, or a scrambled control (Dharmacon) for 24 h before other treatments.

The following primary antibodies were used: UBE3A (Sigma, E8655), SK2 (Gift from Dr. Adelman) (Bond et al., 2004), SK2 (Alomone, APC-028), SK2 (Aviva, ARP35094-T100), SK2 (Santa Cruz, sc-101991), PSD95 (Thermo, MA1-045), synaptophysin (Millipore, MAB-368), ubiquitin (Ub, Sigma, U0508), Ub (Santa Cruz, sc-9133), Tac7G7 (7G7B6, ATCC, HB-8784), Tac (R&D Systems, AB-223-NA), HA (Sigma, H9658), GluA1 (Millipore, 04-855), and β-actin (Sigma, A5441). All secondary antibodies for western blots were obtained from LI-COR, and

for immunofluorescence Alexa-488, -555 and -594 conjugated secondary antibodies were obtained from Invitrogen.

Immunoprecipitation and Denaturing Immunoprecipitation

For immunoprecipitation of SK2 or UBE3A, proteins from hippocampal crude synaptosomal fractions, rabbit anti-SK2 antibodies (Santa Cruz) or mouse anti-UBE3A antibodies, were incubated with P2 lysates and precipitated with Protein A/G-conjugated beads (Pierce). Inputs and precipitates were resolved by SDS-PAGE and analyzed by Western blotting. All studies were performed in 3-5 independent experiments.

For immunoprecipitation of SK2 from hippocampal crude synaptosomal fractions under denaturing conditions, P2 pellets were resuspended and heated in denaturing lysis buffer (1 % SDS, 50 mM Tris, pH 7.4, 5 mM EDTA, 10 mM DTT, 1 mM PMSF, 2 μg/ml leupeptin, 15 U/ml DNase I) and diluted in 9 volumes of ice-cold non-denaturing lysis buffer (1 % Triton X-100, 50 mM Tris, pH 7.4, 300 mM NaCl, 5 mM EDTA, 10 mM iodoacetamide, 1 mM PMSF, 2 μg/ml leupeptin). Lysates were centrifuged at 16,000 g for 30 min at 4 °C and cleared with protein A/ G Agarose beads. Pre-cleared lysates were then incubated with antibodies (anti-SK2, Alomone) coupled to protein A/G Agarose beads overnight at 4°C, followed by four washes with ice-cold wash buffer (0.1 % Triton X-100, 50 mM Tris, pH 7.4, 300 mM NaCl, 5 mM EDTA) and elution in 2 X SDS sample buffer. Immunoprecipitated proteins were resolved by SDS-PAGE followed by Western blot analysis with specific antibodies against SK2 and ubiquitin. At least three independent experiments were performed.

His-ubiquitin Pull-down Assay

COS-1 cells were transfected with His-ubiquitin plus Tac-SK2 or ΔK, and HA-UBE3A or HA-UBE3A C833A constructs, or UBE3A or control siRNA. Twenty-four hours after transfection,

cells were lysed, and His-ubiquitin-conjugated proteins were purified as described (Xirodimas et al., 2001), with minor modifications. Briefly, cells were lysed in Buffer A (6 M guanidine HCl, 0.1 M Na_2HPO_4/NaH_2PO_4, 0.5 M NaCl, 10 mM imidazole, 0.1 % Nonidet P-40, and 5 % glycerol, pH 8.0) and sonicated. The guanidine lysates were then incubated with Talon resin at 4 °C for 4 h to bind His-tagged ubiquitinated proteins. Beads were then washed one time with Buffer A, followed by four washes with Buffer B (8 M urea, 0.1 M Na_2HPO_4/NaH_2PO_4, 0.5 M NaCl, 20 mM imidazole, 0.1 % Nonidet P-40, and 5 % glycerol, pH 8.0). The protein conjugates were eluted in 2 X Laemmli/imidazole (200 mM imidazole) and boiled. At least three independent experiments were performed.

In Silico Molecular Docking

In silico molecular docking was performed between SK2 LZ domain and E3 ligase UBE3A in order to elucidate the potential binding pose and the role of lysine residues in SK2 C-terminal. A crystal structure of SK2 C-term helix (PDB ID 2PNV, chain A 488 to 526) (Kim et al., 2008) and the crystal structure of UBE3A (PDB ID 1D5F) (Huang et al., 1999) were used for docking. Patchdock (Duhovny D, 2002; Schneidman-Duhovny et al., 2005) was used for docking the two rigid protein segments using shape complementarity criteria. The docking results were clustered based on root-mean-square deviation of atomic positions less than 2 Å. The top 100 binding poses were further optimized using FireDock (Huang et al., 1999; Kim et al., 2008), which is designed for interaction refinement in protein-protein docking. The top binding pose after refinement is shown in Fig. 3D.

Endocytosis Assay of Tac-SK2 in COS-1 Cells

Analysis of Tac-SK2 internalization was performed as previously reported (Roche et al., 2001; Standley et al., 2000). In brief, transiently transfected COS-1 cells, plated on glass

coverslips, were washed with ice-cold PBS, incubated with Tac7G7 antibodies for 1 h at 4 °C to label surface Tac, and transferred to the 37 °C incubator for 15 min to allow internalization. After fixation with 4% paraformaldehyde/4% sucrose in PBS, cells were washed and incubated with Alexa 488-conjugated secondary antibodies to visualize the remaining surface Tac-SK2 proteins. Cells were then permeabilized with 0.25% Triton X-100 and internalized Tac-SK2 proteins were detected with an Alexa 594-conjugated secondary antibodies.

Image Analysis and Quantification

Cells were imaged using a Nikon C1 confocal laser-scanning microscope with a 60 X objective. Images for all groups in a particular experiment were obtained using identical acquisition parameters and analyzed using ImageJ software (NIH). All immunostaining studies were performed in 3-5 independent experiments. In all cases the experimenter was blind regarding the identity of the transfected constructs during acquisition and analysis. For endocytosis assay of Tac-SK2, cells were randomly chosen among those that were well separated and showed surface Tac staining. To avoid bias, cell selection was performed in the green channel (surface-expressed) before analysis of internalization (red channel). After background subtraction, signals of internalized puncta and surface-expressed were quantified by manually outlining individual cells and measuring fluorescence intensity. Surface expression was defined as mean fluorescence of surface-expressed normalized to total cellular area. Internalization was scored by calculating internalized over total (surface + internalized) ratios. ‘‘N’’ refers to the number of microscopic fields (each containing 3–5 analyzable COS-1 cells). In each experiment, cells transfected with the Tac constructs but kept at 4 °C to arrest trafficking were included as negative controls.

Neuronal Biotinylation Assay

High-density hippocampal neurons prepared from WT or AS mice and cultured for 12-14 days in vitro were incubated with 100 µg/ml of the lysosomal protease inhibitor leupeptin for 1 h before biotinylation with 1.5 mg/ml sulfo-NHS-SS-biotin (Pierce) for 12 min at 4 °C (Roche et al., 2001). Neurons were then incubated for 30 min at either 4 °C to block membrane trafficking or 37 °C to allow endocytosis to occur. The remaining surface biotin was then cleaved by reducing its disulfide linkage with glutathione cleavage buffer (50 mM glutathione in 75 mM NaCl and 10 mM EDTA containing 1% BSA and 0.075 N NaOH) twice for 15 min at 4 °C. Another sister dish was used to control for the efficacy of the biotin stripping protocol. Cell membranes were prepared, and biotinylated proteins were precipitated with NeutrAvidin Agarose (Pierce) as described (Arancibia-Carcamo et al., 2006).

Acute Hippocampal Slice Preparation, Electrophysiology, and Phalloidin Staining

Acute hippocampal transversal slices (400 µm-thick) were prepared from adult male mice (2-4-month-old) as previously described (Baudry et al., 2012) and recording was done in an interface recording chamber; slices were continuously perfused with oxygenated (95 % O_2/5 % CO_2) and preheated (33 ± 0.5 °C) artificial cerebrospinal fluid (aCSF) (in mM) [110 NaCl, 5 KCl, 2.5 $CaCl_2$, 1.5 $MgSO_4$, 1.24 KH_2PO_4, 10 D-glucose, 27.4 $NaHCO_3$]. Field EPSPs (fEPSPs) were elicited by stimulation of the Schaffer collateral pathway in CA1 stratum radiatum. Before each experiment, the input/output (I/O) relation was examined by varying the intensity of the stimulation. Long-term potentiation was induced using theta burst stimulation (10 bursts at 5 Hz, each burst consisting of 4 pulses at 100 Hz). Long-term depression was induced by 900 pulses delivered at 1 Hz. Synaptic NMDA receptor-mediated responses were obtained using Mg^{2+}-free aCSF containing 10 µM NBQX. Data were collected

and digitized by Clampex; the slope of fEPSP was analyzed in most of the experiments, except for NMDA receptor-mediated responses in which the amplitude of fEPSP was analyzed. All data are expressed as means ± S.E.M., and statistical significance of differences between means was calculated with appropriate statistical tests as indicated in figure legends. Phalloidin staining of F-actin was performed as previously described (Baudry et al., 2012; Wang et al., 2014). All images were taken in CA1 stratum radiatum between the stimulating and recording electrodes.

Immunofluorescence of Brain Tissue Sections

For immunofluorescence brain sections (25 μm) were stained as previously described (Sun et al., 2015; Wang et al., 2014). Images were acquired using Nikon C1 confocal laser-scanning microscope. All analysis and quantifications were performed using the NIH Image J software. The apical dendrites in the CA1 region of hippocampus were randomly selected for puncta analysis. Four-six mice were used for each genotype; 6-8 regions of interest and over 500 particles were analyzed for each mouse. The number and size of SK2-, PSD95- and synaptophysin-stained puncta were quantified and the percentage of SK2 and PSD95 or SK2 and synaptophysin dually stained synapses were also analyzed.

Fear Conditioning

AS mice and their WT littermates were randomly assigned to either drug or vehicle groups and blinded to the examiner. Mice were injected intraperitoneally (i.p.) with apamin (0.4 mg/kg body weight) 30 min before being placed in the fear-conditioning chamber (H10-11M-TC, Coulbourn Instruments). The conditioning chamber was cleaned with 10% ethanol to provide a background odor. A ventilation fan provided a background noise at ~55 dB. After a 2 min exploration period, three tone-footshock pairings separated by 1 min intervals

were delivered. The 85 dB 2 kHz tone lasted 30 s and co-terminated with a footshock of 0.75 mA and 2 s. Mice remained in the training chamber for another 30 s before being returned to home cages. Context test was performed one day after training in the original conditioning chamber with 5 min recording. On day three, animals were subjected to cue/tone test in a modified chamber with different texture and color, odor, background noise, and lighting. After 5 min recording, mice was exposed to a tone (85 dB, 2 kHz) for 1 min. Mouse behavior was recorded with the Freezeframe software and data were analyzed using the Freezeview software (Coulbourn Instruments). Motionless bouts lasting more than 1 s were considered as freezing. The percent of time animal froze was calculated and group means with S.E.M. and cumulative distribution of % freezing were analyzed.

Supplemental References

Arancibia-Carcamo, I.L., Fairfax, B.P., Moss, S.J., and Kittler, J.T. (2006). Studying the Localization, Surface Stability and Endocytosis of Neurotransmitter Receptors by Antibody Labeling and Biotinylation Approaches. In The Dynamic Synapse: Molecular Methods in Ionotropic Receptor Biology, J.T. Kittler, and S.J. Moss, eds. (Boca Raton (FL)).

Bond, C.T., Herson, P.S., Strassmaier, T., Hammond, R., Stackman, R., Maylie, J., and Adelman, J.P. (2004). Small conductance Ca2+-activated K+ channel knock-out mice reveal the identity of calcium-dependent afterhyperpolarization currents. The Journal of neuroscience : the official journal of the Society for Neuroscience *24*, 5301-5306.

Strassmaier, T., Bond, C.T., Sailer, C.A., Knaus, H.G., Maylie, J., and Adelman, J.P. (2005). A novel isoform of SK2 assembles with other SK subunits in mouse brain. The Journal of biological chemistry *280*, 21231-21236.

Talis, A.L., Huibregtse, J.M., and Howley, P.M. (1998). The role of E6AP in the regulation of p53 protein levels in human papillomavirus (HPV)-positive and HPV-negative cells. The Journal of biological chemistry *273*, 6439-6445.